PUBLISHED VERSION

Stevenson, Mark Andrew; Lohmann, Birgit

Fully differential cross-section measurements for electron-impact ionization of argon over the complete in-plane angular range Physical Review A, 2008; 77(3):032708

© 2008 American Physical Society

http://link.aps.org/doi/10.1103/PhysRevA.77.032708

PERMISSIONS

http://publish.aps.org/authors/transfer-of-copyright-agreement

"The author(s), and in the case of a Work Made For Hire, as defined in the U.S. Copyright Act, 17 U.S.C.

§101, the employer named [below], shall have the following rights (the "Author Rights"):

[...]

3. The right to use all or part of the Article, including the APS-prepared version without revision or modification, on the author(s)' web home page or employer's website and to make copies of all or part of the Article, including the APS-prepared version without revision or modification, for the author(s)' and/or the employer's use for educational or research purposes."

21th March 2013

http://hdl.handle.net/2440/45506

Fully differential cross-section measurements for electron-impact ionization of argon over the complete in-plane angular range

M. A. Stevenson and B. Lohmann
ARC Centre of Excellence for Antimatter-Matter Studies, The University of Adelaide, Adelaide, SA 5005, Australia
(Received 15 November 2007; published 14 March 2008)

The triple differential cross section for electron-impact ionization of the $3p$ orbital of argon by 113.5 eV incident electrons has been measured using a magnetic angle changer in a conventional $(e,2e)$ spectrometer. Results are presented for 2 eV ejected electrons over an extended angular range, and over the complete coplanar scattering plane for 5 eV ejected electrons. The data reveal previously unobserved structures, and are compared with recent distorted-wave Born approximation (DWBA) and hybrid DWBA R-matrix calculations. Large discrepancies exist between experiment and both calculations in the accessed regions.

DOI: 10.1103/PhysRevA.77.032708 PACS number(s): 34.80.Dp

INTRODUCTION

Electron-impact ionization is a fundamental process in atomic physics, and plays a key role in many naturally occurring phenomena and technological processes. Kinematically complete studies of electron-impact ionization can be obtained using the $(e,2e)$ technique, where both electrons emerging in the final state are detected in coincidence. In doing so, all electron momenta are determined and a cross section, fully differential with respect to all angles and energies is obtained [referred to as the triple differential cross section (TDCS)]. Since this technique was first employed over forty years ago [1], it has been used as a sensitive probe of the structure of the ionized target [2], or of the dynamics of the ionization process [3]. A broad array of data now exists for ionization of fundamental systems such as hydrogen and helium, as well as a range of more complex atomic and molecular targets [4], surfaces [5], and clusters [6]. Beyond direct ionization, more complex processes such as double ionization [7] simultaneous excitation-ionization [8], excitation-autoionization [9], and ionization with Auger emission [10] have also been investigated.

In the last decade, significant progress has been made in this field. On the experimental side, advances in technology such as microchannel plate detectors have enabled the development of a range of multiparameter spectrometers. For example, extension of the COLTRIMS technique to the kinematically complete study of particle impact ionization (the so-called "reaction microscope" [11]), has provided measurements of electron emission distributions for ionization of helium over the complete 4π scattering sphere [12]. This technique is presently being extended to more complex atomic and molecular targets. Alternatively, multiangle multienergy detectors based around toroidal analyzers have provided insight into the finer details of the ionization process [13,14]. Such techniques employ greater data collection efficiency, enabling a more detailed investigation of the complex ionization processes discussed earlier [15,16], which were previously hampered by very small signal rates.

On the theoretical side, a breakthrough came with the exact solution of the electron-hydrogen scattering problem, using numerical methods such as exterior complex scaling (ECS) [17] or convergent close coupling (CCC) [18]. These methods, although computationally intensive, have also been successfully applied to helium [19,20], but the complexity of describing heavier noble gas targets using these models has prevented application of these approaches to such targets. The most successful alternative is the distorted-wave Born approximation (DWBA). This can reasonably reproduce TDCS for incident energies of 200 eV or above [21], without being restricted to simple targets. For comparison, experimental data over a range of kinematics and geometries is available for the noble gases, and several modifications to the DWBA have been implemented to improve agreement. A comprehensive review of the application of this method to valence and inner valence ionization of noble gases can be found in Ref. [22].

At lower incident ($<$200 eV) and ejected electron energies, a multitude of physical processes become significant, one of which is the Coulomb repulsion between scattered and ejected electrons in the final state. This effect, often referred to as post collision interaction (PCI), is only treated to first order in a standard DWBA code. Another important effect is the increased likelihood of electrons to exchange with each other. In the final state, the ejected electron can exchange with the scattered electron or any of the remaining target electrons. The latter is referred to as exchange distortion due to its effect on the continuum wave function [22]. In the initial state, the projectile may also exchange with any of the target electrons, but this process is commonly assumed to be negligible at the energy range considered in this paper.

Recent experimental work has been undertaken to study low-energy ionization of both valence and inner valence orbitals of argon. For inner valence ionization, the study of Haynes and Lohmann [23] used an incident energy of 113.5 eV with ejected electron energies of 2–10 eV, where effects such as PCI and exchange should have a significant role. The experiments were performed in coplanar asymmetric kinematics, in which the high-energy scattered electron is detected at a fixed forward angle of 15°, and the slow ejected electrons are detected in the scattering plane. A comparative study under similar kinematics was undertaken by Haynes and Lohmann [24] for ionization of the outer $3p$ orbital, and was later extended to 200 eV incident energy by Stevenson *et al.* [25]. These studies highlighted significant discrepancies between experiment and available theories, and pro-

 ©2008 The American Physical Society

voked further theoretical investigations into the problem. In the work of Ref. [22], two improved theoretical models were presented describing the experimental data of Refs. [23–25], considering both valence and inner valence shell ionization. In the first model, a DWBA-based code was modified to include PCI to an infinite order of perturbation theory by including the Coulomb interaction directly in the final state. The second model employed a hybrid DWBA R-matrix method, which described the slow ejected electron by a close coupling approach. The latter calculation includes exchange distortion properly for the slower electron, and hence may be expected to do well when the excess energy is shared in a highly asymmetric way between the two final state electrons [22]. This method was developed further in Ref. [26], where the effects of channel coupling and target structure were investigated. As the two theoretical approaches described above differ in the extent to which they include the effects of PCI and exchange, comparison of the experimental results with the two calculations can provide information on the relative importance of these effects. Although the earlier studies illustrated the importance of proper treatment of exchange and PCI for describing this ionization process, discrepancies between theory and experiment still exist for both models.

Although significant theoretical improvements were made, it was often suggested that experimental data over an increased angular range would provide further guidance for theoretical developments. Due to the relative position of detectors and electron gun, the $(e,2e)$ spectrometer used in the present study is typically limited to detection of ejected electrons in the angular ranges $45°-135°$ and $225°-285°$ for the chosen geometry and kinematics. Although this range is often sufficient to cover all major features for higher energy studies of simple targets, the calculated TDCS in the kinematical range for the target considered here show significant structure outside the available range of conventional spectrometers. To this end, we have incorporated a magnetic angle changing device (MAC) developed by Read and Channing [27] into an $(e,2e)$ spectrometer to increase the angular coverage. This technique was first employed by our group to study inner valence ionization of argon under similar kinematics to those in the present study [28]. In the present work, the data of Ref. [24] was extended over the backward scattering direction, resolving features which were inaccessible in the previous experiment.

In this paper, we present TDCS data for ionization of the $3p$ orbital of argon by 113.5 eV incident electrons, for ejected electron energies of 2 and 5 eV. The data of Ref. [24] is extended over an increased angular range for an ejected energy of 2 eV, and extended to cover the complete 360° coplanar scattering angular range for an ejected energy of 5 eV. We believe this to be the first published measurement over the full coplanar angular range obtained using a conventional $(e,2e)$ spectrometer.

EXPERIMENTAL APPARATUS

The $(e,2e)$ spectrometer has been described in detail in a previous publication [23]. Briefly, a six-element electrostatic lens system with hairpin tungsten filament is used to produce a monoenergetic beam of electrons of around 0.5 eV full width at half maximum (FWHM) energy spread. This intersects an atomic gas jet produced from a stainless steel capillary, of 0.7 mm diameter, at right angles. This "interaction region" is at the center of two independently rotatable turntables, driven by stepper motors. Identical energy selective electron analyzers are mounted on each of the two turntables. Each energy analyzer comprises a four-element input lens system and hemispherical electrostatic energy selector. Electrons are detected at the hemisphere exit aperture using a channel electron multiplier, and are processed using conventional fast timing electronics in the coincident detection of scattered/ejected electrons. The overall resolution in coincidence mode is around 0.75 eV FWHM. The spectrometer is housed in a stainless steel vacuum chamber maintained at a base pressure of 2×10^{-7} Torr. A combination of mu metal shielding and Helmholtz coils is used to reduce the Earth's magnetic field to less than 5 mG. All data collection is undertaken under computer control, with each angular range scanned over several times to reduce scatter in the data due to random fluctuations.

Details of the technique using an $(e,2e)$ spectrometer equipped with a MAC have also been discussed in detail in a previous paper [28]. A uniform magnetic field, created at the interaction region using a system of solenoids, is used to deflect ejected electrons from inaccessible to accessible regions of the scattering plane. Two coaxial pairs of solenoids, consisting of an inner pair and an outer pair, are used to generate the field. The upper and lower coils of each pair are separated by a gap which exposes the interaction region to the electron gun and electron detectors. The use of inner and outer solenoids ensures that the electrons always pass through the interaction region and emerge in a radial direction, independent of the deflection used. By a careful selection of geometry and balancing of inner and outer solenoid currents, low order magnetic multipole moments are cancelled out and the field decreases rapidly outside the MAC. This leaves a field free region at the analyzer entrance and localizes the field to inside the device. From the empirical determination of constants used in the equation for calculating deflections, we estimate the error in the determination of the angular deflection produced by the MAC to be $+/-5°$.

Even though the incident, scattered and ejected electrons all undergo deflection, in the highly asymmetric energy sharing kinematics studied the ejected electrons will undergo a much greater deflection than the incident/scattered electrons. As discussed in Ref. [28], if the field direction is chosen to rotate the ejected electron distribution anticlockwise with respect to the incident beam, the direction of the scattered beam is also rotated anticlockwise. Since the lower angular range of the ejected electron analyzer is usually limited by the position of the scattered electron analyzer, this has the advantage of increasing the accessible angular range of the ejected electron analyzer. However, if the deflection is chosen to be clockwise, the accessible angular range is decreased.

For measurements in the region $135°-225°$, an anticlockwise deflection was used, thus increasing the angular range. This was advantageous in increasing the overlap with exist-

ing data for normalization purposes. Covering the range from 135°–225° in one go was theoretically possible, but required large deflections which have proved problematic. Instead, this region was measured in two parts by deflecting both the binary and recoil region and overlapping and normalizing the two new data sets with each other and the old data.

Measurements over the region from 285° to 360° (i.e., 0°) and on through to 45° required a clockwise deflection, thus decreasing the angular range. This disadvantage is compounded by the fact that the loss is in the unmeasured side of the accessible range, as opposed to the region overlapping the existing data. Thus, measuring this region presents significantly more difficulty than measuring the region 135°–225°. This is evident in the experimental data in this region which, because of the need of good overlap between data sets for normalization, consists of several increasingly smaller data sets. At an ejected energy of 2 eV, we found that it was not possible to perform measurements linking the regions from 335° through to 15°. This is a result of the very large deflection, and hence magnetic field required to access this region. This resulted in sufficient penetration of the magnetic field to perturb the trajectories of the electrons into the analyzers. However, for 5 eV ejected electrons, we were reliably able to operate the MAC over the entire angular region, with good overlap over all data sets.

RESULTS AND DISCUSSION

The measured data of Ref. [24], along with the new data over an extended range can be seen in Figs. 1 and 2. The cross sections were measured in coplanar geometry, under asymmetric energy sharing kinematics. The scattered electrons were detected at a fixed scattering angle of $\theta_a = -15°(345°)$. TDCS were measured as a function of in plane ejected electron angle for an incident energy of 113.5 eV, and ejected energies of 5 and 2 eV. The scattered electron energy was determined by conservation of energy, given by

$$E_0 = E_a + E_b + \varepsilon_i,$$

where E_0 is the incident electron energy, E_a and E_b are the scattered and ejected electron energies respectively, and ε_i is the binding energy of the $3p$ orbital in argon (15.76 eV). The error bars are statistical and represent one standard deviation. We note that the measured data are relative, and not absolute, hence the magnitude of the cross section is not determined. Comparison with the theoretical cross section calculations described below is facilitated by normalizing the experimental data to the calculated cross sections at the main peak in the binary region. In order to combine the different data sets corresponding to different deflections in the magnetic angle changer, measurements over different angular ranges overlap each other significantly. The overlap regions are then normalized to give best visual fit over the entire overlapping region. In cases where the overlap region is large, or where a particular data set overlaps two other data sets at the low end and the high end of the angular range, this process is quite robust. It is less reliable when there are only a few overlap points.

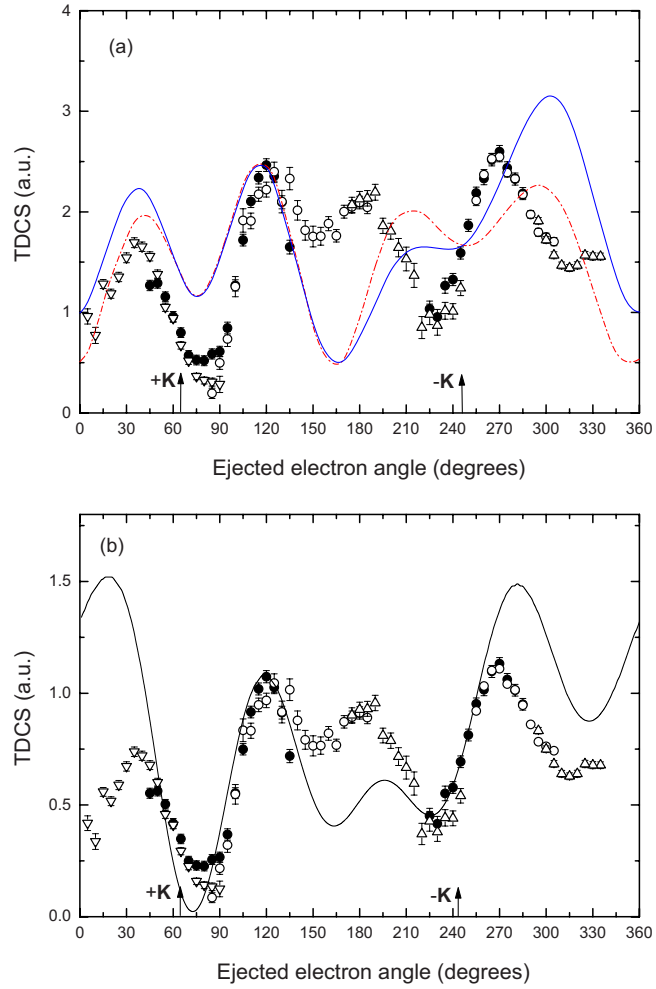

FIG. 1. (Color online) Measured and calculated triple differential cross sections for electron-impact ionization of the $3p$ orbital of argon. The kinematic conditions were E_0=113.5 eV, θ_a=−15°, and E_b=2 eV. The solid circles are the original experimental data from Ref. [24], and the open shapes are the new results obtained with the magnetic angle changer. (a) The dashed curve is the 3DW calculation, and the solid curve is the DW calculation. (b) The solid curve is the DW2 two-state-MC calculation.

Included with our data are the recent calculations of Refs. [22,27] discussed earlier, which approach exchange and/or PCI in different ways. A standard DWBA calculation in which PCI is treated only to the first order is included, denoted by DW [22]. This calculation is then extended by including a Coulomb distortion factor directly in the final state wave function. In doing so, the scattered electron-ion, ejected electron-ion and scattered electron-ejected electron Coulomb interactions are accounted for to all orders of perturbation theory. This approach was pioneered by Brauner, Briggs, and Klar [29]; in their work the incident and outgoing waves were described as Coulomb waves. However, as Coulomb waves are inaccurate for heavier targets, distorted wave descriptions for the incident and two outgoing electrons are used instead. Henceforth, this model is referred to as 3DW (three distorted wave). The DW and 3DW calculations do not include exchange between the incident projectile

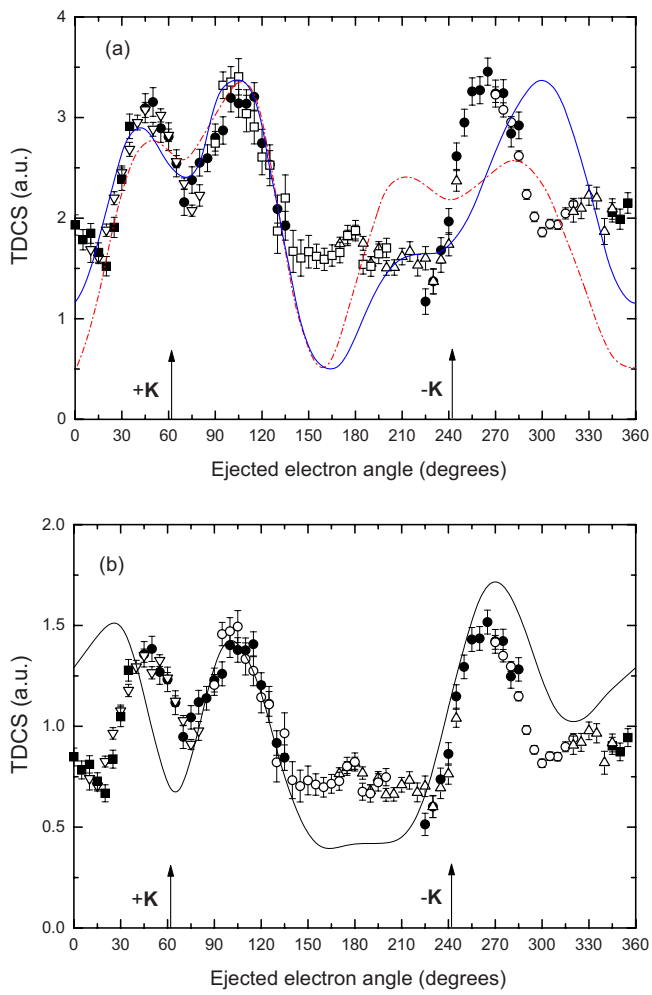

FIG. 2. (Color online) Measured and calculated triple differential cross sections for electron-impact ionization of the $3p$ orbital of argon. The kinematic conditions were $E_0=113.5$ eV, $\theta_a=-15°$, and $E_b=5$ eV. The solid circles are the original experimental data from Ref. [24], and the solid squares and open shapes are the new results obtained with the magnetic angle changer. (a) The dashed curve is the 3DW calculation, and the solid curve is the DW calculation. (b) The solid curve is the DW2 two-state-MC calculation.

and the target electrons, or between the ejected electron and the remaining target electrons. An attempt to incorporate this exchange effect into the DW and 3DW models was made in Ref. [22]. Although this improved agreement with the recoil peak at lower ejected energies, those calculations do not reproduce the binary peak shape well and are not included here.

For the hybrid DWBA R-matrix calculation the incident and scattered electrons are described by a second order DWBA (DWB2), whereas the ejected electron-residual ion scattering process is modeled by an R matrix (close coupling) expansion. This treatment accounts for exchange between the ejected electron and the residual ion, whereas projectile-target exchange is neglected. The inner valence $3s$ and outer $3p$ orbital ionization channels are coupled, however the effects of channel coupling in this calculation were shown to be small for outer shell ionization [27]. To account for configuration mixing, the initial bound state and final ionic state are described by a multiconfiguration (MC) expansion. Hence, the calculation is referred to in Ref. [27], and in this paper as DWB2 two-state-MC. This calculation cannot incorporate PCI effects at this time.

The results for an ejected electron energy of 2 and 5 eV, respectively, are presented in Figs. 1 and 2. In Figs. 1(a) and 2(a) our experimental data are compared with the DW and 3DW calculations, while in Figs. 1(b) and 2(b) they are compared with the DWB2 two-state-MC. The experimental data consists of a number of data sets, overlapping in angle; different data sets are represented by different symbols. The cross sections may be conveniently described in terms of their structure in the binary region $(0°-180°)$ and the recoil region $(180°-360°)$. The momentum transfer direction $\mathbf{K}$ and $-\mathbf{K}$ are also shown in the figures. The momentum transfer is defined as $\mathbf{K}=\mathbf{k}_o-\mathbf{k}_a$, where $\mathbf{k}_o$ is the momentum vector of the incident electron and $\mathbf{k}_a$ is that of the scattered electron. The experimental data have been normalized to the various theories in the region of the second binary peak. For an ejected electron energy of 2 eV (Fig. 1), comparison with the DW and 3DW calculations shows that the binary region of the cross section is reasonably well represented by both calculations, although the depth of the minimum near the momentum transfer direction is underestimated. The double-peak structure in the binary region is indicative of ionization by a p orbital. There is some difference in the predicted magnitude of the first peak in the binary region, with the 3DW being in somewhat better agreement with the observed relative magnitude of the two peaks in this region. Both calculations, however, predict the peak positions very well. In contrast, the agreement in the recoil region of the cross section is much poorer. The extended experimental angular range has allowed us to resolve the position of the main peak structure in the recoil region, at 270°, and to fill in the region between 140° and 220°; the results show another smaller peak structure in this region. Although the DW and 3DW calculations predict this two peak structure, the agreement with experiment in terms of the position of the peaks is very poor. In the calculations, the dip between the two peaks is centered on the $-\mathbf{K}$ direction. As the recoil structure in these kinematics is attributed to the elastic backscattering of the ejected electron from the residual ion, it is possible that remnants of the double binary peak structure (due to ionization of a p orbital) may be "mapped" into the recoil region. Alignment of the dip between the two peaks with the $-\mathbf{K}$ direction is consistent with this interpretation. However, the experimental data show that the peak positions are quite different to those predicted in the calculation, suggesting that other effects are important in producing the observed behavior. We note that there is little difference in the peak positions predicted by the DW compared with the 3DW, suggesting that PCI is not responsible for the observed difference in peak positions. However, there is a significant difference in the magnitude of the second recoil peak in the 3DW calculation, with it being substantially reduced as a result of the inclusion of the final state Coulomb repulsion.

In Fig. 1(b), the experimental data are compared with the DWB2 two-state-MC calculation. The latter calculation predicts the correct general structure of the cross section, with a

deep dip between the two binary peaks, and a two peak structure in the recoil region. The angular position of a number of the structures in this case are well predicted by the theory. The notable differences are in the magnitude of the first binary peak, and of the two recoil peaks. Bearing in mind that this calculation does not include post-collision interaction in any form, and noting that the inclusion of long-range Coulomb effects exactly in the 3DW resulted in a reduction in the magnitudes of these features, one may conclude that this discrepancy could be partially resolved by inclusion of PCI. Of interest is the feature around 170° in the experimental cross section; this structure is considerably enhanced compared with the peak predicted in the DWB2 two-state-MC, and appears at a lower angle. This region corresponds roughly to the angular position where the two electrons would emerge back-to-back, and it is possible that the enhancement of the cross section reflects a preference for back-to-back emission.

The experimental and theoretical results for emission of a 5 eV electron are shown in Fig. 2. Similar observations may be made regarding the level of agreement between experiment and the various theories for this case. The DW and 3DW predict the binary region very well for this case, but there is significant disagreement in the recoil region. The DWB2 two-state-MC predicts the general features of the cross section well, with the exception of the forward angle binary peak, which appears at too low an angle. The discrepancy between the calculated and experimental magnitudes of the first binary peak and second recoil peak is not as great as for 2 eV, probably indicating that the effect of PCI is smaller in this case. This is also borne out by the reduced differences between the 3DW and DW results. The DWB2 two-state-MC calculation predicts a very small structure around 180°; such a structure is also seen in the experimental results, again around 170° and again enhanced compared with the theoretically predicted peak. This second recoil peak is, however, considerably smaller than that observed at 2 eV, perhaps due to reduced PCI.

CONCLUSION

The angular range of a conventional $(e,2e)$ spectrometer has now been extended to cover the full coplanar scattering range using a magnetic angle changing device. The data reveal significant structures outside the range of the previous study [24]; comparison with available theoretical calculations illustrates some agreement, but also large discrepancies in the newly accessed regions. The level of agreement between the experimental data and the DW, 3DW and DWB2 two-state-MC calculations is mixed. Inclusion of PCI to all orders in the 3DW calculation indicates that the cross section in the recoil region changes substantially when this effect is included. Therefore, the addition of PCI in the DWB2 two-state-MC calculation may yield much improved agreement.

ACKNOWLEDGMENTS

The support of the Australian Research Council is gratefully acknowledged.

[1] H. Ehrhardt, M. Schulz, T. Tekaat, and K. Willmann, Phys. Rev. Lett. **22**, 89 (1969).
[2] E. Weigold and I. E. McCarthy, *Electron Momentum Spectroscopy* (Kluwer Academic/Plenum, New York, 1999).
[3] A. Lahmam-Bennani, J. Electron Spectrosc. Relat. Phenom. **123**, 365 (2002).
[4] M. Takahashi, N. Watanabe, Y. Khajuria, Y. Udagawa, and J. H. D. Eland, Phys. Rev. Lett. **94**, 213202 (2005).
[5] S. Samarin, O. M. Artamonov, A. D. Sergeant, J. Kirschner, A. Morozov, and J. F. Williams, Phys. Rev. B **70**, 073403 (2004).
[6] M. Vos, S. A. Canney, I. E. McCarthy, S. Utteridge, M. T. Michalewicz, and E. Weigold, Phys. Rev. B **56**, 1309 (1997).
[7] C. Jia, A. Lahmam-Bennani, A. Duguet, L. Avaldi, M. Lecas, and C. Dal Capello, J. Phys. B **35**, 1103 (2002).
[8] S. Bellm, J. Lower, K. Bartschat, X. Guan, D. Weflen, M. Foster, A. L. Harris, and D. H. Madison, Phys. Rev. A **75**, 042704 (2007).
[9] J. Lower and E. Weigold, J. Phys. B **23**, 2819 (1990).
[10] A. Naja, E. M. Staiçu-Casagrande, X. G. Ren, F. Catoire, A. Lahmam-Bennani, C. Dal Capello, and C. T. Whelan, J. Phys. B **40**, 2871 (2007).
[11] R. Moshammer, M. Unverzgat, W. Schmitt, J. Ullrich, and H. Schmidt-Böcking, Nucl. Instrum. Methods Phys. Res. B **108**, 42 (1996).
[12] M. Dürr, C. Dimopoulou, B. Najjari, A. Dorn, and J. Ullrich, Phys. Rev. Lett. **96**, 243202 (2006).
[13] A. Duguet, A. Lahmam-Bennani, M. Lecas, and B. El Marji, Rev. Sci. Instrum. **69**, 3524 (1998).
[14] M. J. Ford, J. P. Doering, J. H. Moore, and M. A. Coplan, Rev. Sci. Instrum. **66**, 3137 (1995).
[15] M. Dürr, A. Dorn, J. Ullrich, S. P. Cao, A. Czasch, A. S. Keifets, J. R. Götz, and J. S. Briggs, Phys. Rev. Lett. **98**, 193201 (2007).
[16] S. Bellm, J. Lower, and K. Bartschat, Phys. Rev. Lett. **96**, 223201 (2006).
[17] T. N. Resigno, M. Baertschy, W. A. Issacs, and C. W. McCurdy, Science **286**, 2474 (1999).
[18] I. Bray, Phys. Rev. Lett. **89**, 273201 (2002).
[19] M. Stevenson, B. Lohmann, I. Bray, D. V. Fursa, and A. T. Stelbovics, Phys. Rev. A **75**, 034701 (2007).
[20] K. Bartschat, I. Bray, D. V. Fursa, and A. T. Stelbovics, Phys. Rev. A **76**, 024703 (2007).
[21] S. Jones, D. H. Madison, and M. Baertschy, Phys. Rev. A **67**, 012703 (2003).
[22] A. Prideaux, D. H. Madison, and K. Bartschat, Phys. Rev. A **72**, 032702 (2005).
[23] M. A. Haynes and B. Lohmann, J. Phys. B **33**, 4711 (2000).
[24] M. A. Haynes and B. Lohmann, Phys. Rev. A **64**, 044701 (2001).
[25] M. Stevenson, G. J. Leighton, A. Crowe, K. Bartschat, O. K.

Vorov, and D. H. Madison, J. Phys. B **38**, 433 (2005).
[26] K. Bartschat and O. Vorov, Phys. Rev. A **72**, 022728 (2005).
[27] F. H. Read and J. M. Channing, Rev. Sci. Instrum. **67**, 2372 (1996).
[28] M. Stevenson and B. Lohmann, Phys. Rev. A **73**, 020701(R) (2006).
[29] M. Brauner, J. S. Briggs, and H. Klar, J. Phys. B **22**, 2265 (1989).